Supplementary information with

MODELLING SALINITY EFFECTS ON AEROBIC GRANULAR SLUDGE TREATING FISH-CANNING WASTEWATER

P. Carrera[a,b*], L. Strubbe[b], A. Val del Río[a], A. Mosquera-Corral[a], E.I.P. Volcke[b]

[a] CRETUS Institute. Department of Chemical Engineering, Universidade de Santiago de Compostela. E-15782, Santiago de Compostela, Spain

[b] BioCo Research Group, Department of Green Chemistry and Technology, Ghent University, Coupure Links 653, 9000 Gent, Belgium

*Corresponding author: Paula Carrera (Paula.CarreraFernandez@UGent.be)

Appendix A. Supplementary data

In this appendix, details of the developed one-dimensional biofilm model are given. They include the data used for the calibration and validation of the model (Appendix A.1), the biological conversion reactions, stoichiometric matrix and kinetic and stoichiometric parameters (Appendix A.2). As for salinity inhibition, a literature review of different non-competitive inhibition terms is given in Appendix A.3, also dealing with, the estimating procedure of the inhibition constants used in the model. Some model calibration results are included in Appendix A.4.

Appendix A.1: Model input data

The experimental data used to calibrate and validate the model corresponds to the reactor operation described by Carrera et al. (2019) and is summarized in Table S.1.

Table S.1. Model input data used for the calibration and validation. Experimental data mentioned in the table can be found in Carrera et al. (Carrera et al., 2019).

Symbol	Definition	Calibration	Validation	Units	Reference
Influent characteristics					
$S_{NHx,in}$	Influent NH_x concentration	73	106	g $N.m^{-3}$	Exp. data
$S_{S,in}$[1]	Influent soluble readily biodegradable COD	440	700	g $COD.m^{-3}$	Exp. data
$S_{I,in}$[1]	Influent soluble inert COD	170	200	g $COD.m^{-3}$	Exp. data
$X_{S,in}$[1]	Influent particulate slowly biodegradable COD	83	34	g $COD.m^{-3}$	Exp. data
$X_{I,in}$[1]	Influent particulate inert COD	87	36	g $COD.m^{-3}$	Exp. data
Granule characteristics					
ε_w	Granule porosity	0.8	0.8	-	De Kreuk et al. (2007)
R_{SS}	Surface mean diameter of granules at steady state	1.25	1.1	mm	Exp. data
ρ[2]	Density of the granules	165	140	g $VSS.m^{-3}$	Exp. data
ρ_{BM}	Density of biomass	1.13×10^6	9.62×10^5	g $COD.m^{-3}$	Calculated (this study)
ρ_{PHA}	Density of PHA	1×10^9	1×10^9	g $COD.m^{-3}$	De Kreuk et al. (2007)
n_g	Number of granules	59593	89000	-	Calculated (this study)
ε_{PHA}	Initial concentration of PHA	0	0	-	Calculated (this study)
ε_{OHO}	Initial concentration of OHO	0.19	0.19	-	Calculated (this study)
ε_{AOB}	Initial concentration of AOB	0.01	0.01	-	Calculated (this study)
ε_{NOB}	Initial concentration of NOB	0	0	-	Calculated (this study)
Reactor and operational conditions					
$V_{reactor}$	Total reactor volume	1.7	1.7	L	Exp. data
VER	Volume exchange ratio	50	50	%	Exp. data
t_{cycle}	Total operation time cycle	4	4	h	Exp. data
$t_{feeding}$	Time of feeding	5	5	min	Exp. data
$t_{settling}$	Time of settling	1	1	min	Exp. data
$t_{discharge}$	Time of discharge	7	7	min	Exp. data
T	Temperature	23	23	°C	Exp. data
S_{O2}	Oxygen concentration	8.6	8.6	g $O_2.m^{-3}$	Exp. data
$VSS_{reactor}$	Sludge concentration in the reactor	5.9	3.6	kg $VSS.m^{-3}$	Exp. data
$ISS_{reactor}/TSS_{reactor}$	Ash content of the reactor	0.16	0.2	kg ISS/kg TSS	Exp. data

[1]The COD fractions were measured through fractionation tests following the procedure described by Cristóvão et al. (2016).

[2]The density of the granules was measured following the procedure described by Beun et al. (2002).

The number of granules in the reactor was calculated based on the volatile suspended solids concentration (X, in g VSS/m^3) and the density of the granules (ρ, in g VSS/m^3), which were both determined experimentally. Granules were assumed to be spherical particles with a uniform radius (R_m), which was taken as the average value measured experimentally. The number of granules was calculated as the ratio between the total volume of granules (V_X, in m^3) and the volume of a single granule (Eq. 1):

$$n_g = \frac{V_X}{{}^4/_3 \pi {R_m}^3} \qquad \text{(Eq.1)}$$

in which

$$V_X = \frac{V_R X}{\rho} \qquad \text{(Eq.2)}$$

Where V_R is the volume of the reactor (m^3) and ρ is the density of the granules (g VSS/m^3, determined experimentally.

The density of the biomass, expressed in terms of COD (ρ_{BM}), was calculated following Eq.3.

$$\rho_{BM} = \rho\left(1 - \frac{ISS_R}{TSS_R}\right)1.3659\left(\frac{1}{1 - \varepsilon_w}\right) \qquad \text{(Eq.3)}$$

Where ρ is the density of the granules (g TSS/m^3, determined experimentally), ISS are the inert suspended solids and TSS the total suspended solids of the reactor, 1.3659 is the ratio COD/VSS of the biomass (g COD/g VSS, Henze et al. (2008)) and ε_W is the porosity of the granules, which was estimated as 0.8 (De Kreuk et al., 2007).

Appendix A.2: model description

In this appendix, a list of the state variables (Table S.2), the stoichiometric matrix (Table S.3), kinetic rate expressions (Table S.4) and stoichiometric and kinetic parameters (Table S.5) are provided.

Table S.2. State variables used in the model

Symbol	Definition	Units
S_{O2}	Dissolved oxygen	g O_2.m^{-3}
S_I	Soluble inert COD	g COD.m^{-3}
S_S	Soluble easily biodegradable COD	g COD.m^{-3}
S_{COD}[1]	Soluble COD (S_I+S_S)	g COD.m^{-3}
S_{NH}	Ammonium and ammonia	g N.m^{-3}
S_{NO2}	Nitrite	g N.m^{-3}
S_{NO3}	Nitrate	g N.m^{-3}
X_I	Particulate inert COD	g COD.m^{-3}
X_S	Particulate slowly biodegradable COD	g COD.m^{-3}
X_H	Heterotrophic organisms	g COD.m^{-3}
X_{STO}	Storage compounds	g COD.m^{-3}
X_A	Ammonia oxidizing bacteria	g COD.m^{-3}
X_N	Nitrite oxidizing bacteria	g COD.m^{-3}

[1]This state variable is not shown in the stoichiometric matrix as it was directly calculated as the sum of S_I and S_S and it was only used to compare the results of the model with experimental data.

Table S.3. Stoichiometric matrix. The highlighted processes correspond to the modifications applied to ASM3: in **blue** heterotrophic growth based on easily biodegradable COD (added to the model to describe simultaneous growth-storage), in **green** two-step nitrification.

		S_{O2}	S_I	S_S	S_{NH}	S_{NO2}	S_{NO3}	X_I	X_S	X_H	X_{STO}	X_A	X_N
Heterotrophic Bacteria													
1	Aerobic hydrolysis		f_{SI}	$1-f_{SI}$	$-i_{NSS}\cdot(1-f_{SI})-(f_{SI}\cdot i_{NSI})+i_{NXS}$				-1				
2	Aerobic storage of Ss	$-(1/Y_{STO}-1)$		$-1/Y_{STO}$							1		
3	Anoxic storage of Ss - NO_2			$-1/Y_{STO}$		$-(1/Y_{STO}-1)/1.71$					1		
4	Anoxic storage of Ss - NO_3			$-1/Y_{STO}$			$-(1/Y_{STO}-1)/2.86$				1		
5	Aerobic growth - Ss	$-(1/Y_H-1)$		$-1/Y_H$	$-i_{NXB}$					1			
6	Anoxic growth - NO_2			$-1/Y_H$	$-i_{NXB}$	$-(1/Y_H-1)/1.71$				1			
7	Anoxic growth - NO_3			$-1/Y_H$	$-i_{NXB}$		$-(1/Y_H-1)/2.86$			1			
8	Aerobic growth - X_{STO}	$-(1/Y_{HSTO}-1)$			$-i_{NXB}$					1	$-1/Y_{HSTO}$		
9	Anoxic growth - NO_2				$-i_{NXB}$	$-(1/Y_{HSTO}-1)/1.71$				1	$-1/Y_{HSTO}$		
10	Anoxic growth - NO_3				$-i_{NXB}$		$-(1/Y_{HSTO}-1)/2.86$			1	$-1/Y_{HSTO}$		
11	Aerobic respiration - Ss	$-(1-f_X)$			$i_{NXB}-i_{XI}\cdot f_X$			f_X		-1			
12	Anoxic endogenous respiration - NO_2				$i_{NXB}-i_{XI}\cdot f_X$	$-(1-f_x)/1.71$		f_X		-1			
13	Anoxic endogenous respiration - NO_3				$i_{NXB}-i_{XI}\cdot f_X$		$-(1-f_x)/2.86$	f_X		-1			
14	Aerobic respiration - X_{STO}	-1									-1		
15	Anoxic respiration of X_{STO} - NO_2					-1/1.71					-1		
16	Anoxic respiration of X_{STO} - NO_3						-1/2.86				-1		

Ammonia Oxidising Bacteria													
17	Aerobic growth	$-(3.43-Y_A)/Y_A$			$-i_{XB}-1/Y_A$	$1/Y_A$						1	
18	Aerobic endogenous respiration	$-(1-f_X)$			$i_{NXB}-i_{XI}\cdot f_X$			f_X				-1	
19	Anoxic endogenous respiration - NO_2				$i_{NXB}-i_{XI}\cdot f_X$	$-(1-f_x)/1.71$		f_X				-1	
20	Anoxic endogenous respiration - NO_3				$i_{NXB}-i_{XI}\cdot f_X$		$-(1-f_x)/2.86$	f_X				-1	
Nitrite Oxidising Bacteria													
21	Aerobic growth	$-(1.14-Y_N)/Y_N$			$-i_{XB}$	$-1/Y_N$	$1/Y_N$						1
22	Aerobic endogenous respiration	$-(1-f_X)$			$i_{NXB}-i_{XI}\cdot f_X$			f_X					-1
23	Anoxic endogenous respiration - NO_2				$i_{NXB}-i_{XI}\cdot f_X$	$-(1-f_x)/1.71$		f_X					-1
24	Anoxic endogenous respiration - NO_3				$i_{NXB}-i_{XI}\cdot f_X$		$-(1-f_x)/2.86$	f_X					-1

Table S.4. Kinetic rate expressions for the bioconversion reactions

1	Hydrolysis	$k_h\left(\frac{X_S/X_{BH}}{K_X+(X_S/X_{BH})}\right)X_H$
Heterotrophic bacteria		
2	Aerobic storage of X_{STO}	$k_{STO}\left(\frac{S_S}{K_{SH}+S_S}\right)\left(\frac{S_O}{K_{OH}+S_O}\right)X_H$
3	Anoxic storage of X_{STO} (NO_2)	$k_{STO}\eta_g\left(\frac{K_{OH}}{K_{OH}+S_O}\right)\left(\frac{S_S}{K_{SH}+S_S}\right)\left(\frac{S_{NO_2}}{K_{NO2H}+S_{NO_2}}\right)X_H$
4	Anoxic storage of X_{STO} (NO_3)	$k_{STO}\eta_g\left(\frac{K_{OH}}{K_{OH}+S_O}\right)\left(\frac{S_S}{K_{SH}+S_S}\right)\left(\frac{S_{NO_3}}{K_{NO3H}+S_{NO_3}}\right)X_H$
5	Aerobic growth on S_S	$\mu_H\left(\frac{K_{Inh,H}}{S_{Inh}+K_{Inh,H}}\right)\left(\frac{S_S}{K_{SH}+S_S}\right)\left(\frac{S_O}{K_{OH}+S_O}\right)\left(\frac{S_{NH}}{K_{NHH}+S_{NH}}\right)X_H$
6	Anoxic growth on S_S NO_2	$\mu_H\eta_g\left(\frac{K_{Inh,H}}{S_{Inh}+K_{Inh,H}}\right)\left(\frac{K_{OH}}{K_{OH}+S_O}\right)\left(\frac{S_S}{K_{SH}+S_S}\right)\left(\frac{S_{NO_2}}{K_{NO2H}+S_{NO_2}}\right)\left(\frac{S_{NH}}{K_{NHH}+S_{NH}}\right)X_H$
7	Anoxic growth on S_S NO_3	$\mu_H\eta_g\left(\frac{K_{Inh,H}}{S_{Inh}+K_{Inh,H}}\right)\left(\frac{K_{OH}}{K_{OH}+S_O}\right)\left(\frac{S_S}{K_{SH}+S_S}\right)\left(\frac{S_{NO_2}}{K_{NO3H}+S_{NO_2}}\right)\left(\frac{S_{NH}}{K_{NHH}+S_{NH}}\right)X_H$
8	Aerobic growth on X_{STO}	$\mu_H\left(\frac{K_{Inh,H}}{S_{Inh}+K_{Inh,H}}\right)\left(\frac{S_O}{K_{OH}+S_O}\right)\left(\frac{S_{NH}}{K_{NHH}+S_{NH}}\right)\left(\frac{X_{STO}/X_{BH}}{K_{STO}+(X_{STO}/X_{BH})}\right)X_H$
9	Anoxic growth on X_{STO} (NO_2)	$\mu_H\eta_g\left(\frac{K_{Inh,H}}{S_{Inh}+K_{Inh,H}}\right)\left(\frac{K_{OH}}{K_{OH}+S_O}\right)\left(\frac{S_{NO_2}}{K_{NO_2}+S_{NO_2}}\right)\left(\frac{S_{NH}}{K_{NHH}+S_{NH}}\right)\left(\frac{X_{STO}/X_{BH}}{K_{STO}+(X_{STO}/X_{BH})}\right)X_H$
10	Anoxic growth on X_{STO} (NO_3)	$\mu_H\eta_g\left(\frac{K_{Inh,H}}{S_{Inh}+K_{Inh,H}}\right)\left(\frac{K_{OH}}{K_{OH}+S_O}\right)\left(\frac{S_{NO_3}}{K_{NO_3}+S_{NO_3}}\right)\left(\frac{S_{NH}}{K_{NHH}+S_{NH}}\right)\left(\frac{X_{STO}/X_{BH}}{K_{STO}+(X_{STO}/X_{BH})}\right)X_H$
11	Aerobic endogenous respiration	$b_H\left(\frac{S_O}{K_{OH}+S_O}\right)X_H$
12	Anoxic endogenous respiration (NO_2)	$b_H\eta_g\left(\frac{K_{OH}}{K_{OH}+S_O}\right)\left(\frac{S_{NO_2}}{K_{NO2N}+S_{NO_2}}\right)X_H$
13	Anoxic endogenous respiration (NO_3)	$b_H\eta_g\left(\frac{K_{OH}}{K_{OH}+S_O}\right)\left(\frac{S_{NO_3}}{K_{NO3N}+S_{NO_3}}\right)X_H$
14	Aerobic endogenous respiration of X_{STO}	$b_{STO}\left(\frac{S_O}{K_{OH}+S_O}\right)X_{STO}$
15	Anoxic endogenous respiration X_{STO} (NO_2)	$b_{STO}\eta_g\left(\frac{K_{OH}}{K_{OH}+S_O}\right)\left(\frac{S_{NO_2}}{K_{NO2N}+S_{NO_2}}\right)X_{STO}$
16	Anoxic endogenous respiration X_{STO} (NO_3)	$b_{STO}\eta_g\left(\frac{K_{OH}}{K_{OH}+S_O}\right)\left(\frac{S_{NO_3}}{K_{NO3N}+S_{NO_3}}\right)X_{STO}$
Ammonia oxidizing bacteria (AOB)		

17	Aerobic growth AOB	$\mu_A\left(\frac{K_{Inh,A}}{S_{Inh}+K_{Inh,A}}\right)\left(\frac{S_{NH}}{K_{NHA}+S_{NH}}\right)\left(\frac{S_O}{K_{OA}+S_O}\right)X_A$
18	Aerobic endogenous respiration	$b_A\left(\frac{S_O}{K_{OA}+S_O}\right)X_A$
19	Anoxic endogenous respiration (NO_2)	$b_A\eta_g\left(\frac{K_{OA}}{K_{OA}+S_O}\right)\left(\frac{S_{NO_2}}{K_{NO2A}+S_{NO_2}}\right)X_A$
20	Anoxic endogenous respiration (NO_3)	$b_A\eta_g\left(\frac{K_{OA}}{K_{OA}+S_O}\right)\left(\frac{S_{NO_3}}{K_{NO2A}+S_{NO_3}}\right)X_A$
Nitrite oxidizing bacteria (NOB)		
21	Aerobic growth NOB	$\mu_N\left(\frac{K_{Inh,N}}{S_{Inh}+K_{Inh,N}}\right)\left(\frac{S_{NO_2}}{K_{NO2N}+S_{NO_2}}\right)\left(\frac{S_O}{K_{ON}+S_O}\right)X_N$
22	Aerobic endogenous respiration	$b_N\left(\frac{S_O}{K_{ON}+S_O}\right)X_N$
23	Anoxic endogenous respiration (NO_2)	$b_N\eta_g\left(\frac{K_{ON}}{K_{ON}+S_O}\right)\left(\frac{S_{NO_2}}{K_{NO2N}+S_{NO_2}}\right)X_N$
24	Anoxic endogenous respiration (NO_3)	$b_N\eta_g\left(\frac{K_{ON}}{K_{ON}+S_O}\right)\left(\frac{S_{NO_3}}{K_{NO3N}+S_{NO_3}}\right)X_N$

Table S.5. Kinetic and stoichiometric parameters

Stoichiometric parameters

Symbol	**Definition**	**Value**	**Units**	**Reference**
Y_A	AOB yield	0.18	kg COD·kg COD	Vázquez-Padín et al. (2010)
Y_N	NOB yield	0.08	kg COD·kg COD	Vázquez-Padín et al. (2010)
Y_{STO}	Yield for storage substrate	0.8	kg COD·kg COD	Vázquez-Padín et al. (2010)
Y_{HSTO}	Heterotrophic yield from X_{STO}	0.68	kg COD·kg COD	Vázquez-Padín et al. (2010)
Y_H	Heterotrophic yield	0.57	kg COD·kg COD	Vázquez-Padín et al. (2010)
f_{SI}	Production of S_I in hydrolysis	0	kg COD·kg COD	Henze et al. (2000)
i_{NXB}	Mass of N per mass of COD in biomass	0.07	g N·(g COD)$^{-1}$	Henze et al. (2000)
i_{NSS}	N content of S_S	0.03	g N·(g COD)$^{-1}$	Henze et al. (2000)
i_{NSI}	N content of S_I	0.01	g N·(g COD)$^{-1}$	Henze et al. (2000)
i_{NXI}	N content of X_I	0.02	g N·(g COD)$^{-1}$	Henze et al. (2000)
i_{NXS}	N content of X_S	0.04	g N·(g COD)$^{-1}$	Henze et al. (2000)

Kinetic parameters

Symbol	**Definition**	**Value**	**Units**	**Reference**
μ_H*	Maximum specific growth rate for heterotrophs	2.46	d^{-1}	Henze et al. (2000)
μ_A*	Maximum specific growth rate for AOB	1.10	d^{-1}	Wiesmann (1994)
μ_N*	Maximum specific growth rate for NOB	1.28	d^{-1}	Wiesmann (1994)
μ_H	Maximum specific growth rate for heterotrophs	**7.76**	d^{-1}	Calibrated - this study
μ_A	Maximum specific growth rate for AOB	**0.27**	d^{-1}	Calibrated – this study
μ_N	Maximum specific growth rate for NOB	**0.16**	d^{-1}	Calibrated – this study
b_H	Decay coefficient for heterotrophs	0.25	d^{-1}	Henze et al. (2000)
b_A	Decay coefficient for AOB	0.074	d^{-1}	Wiesmann (1994)
b_N	Decay coefficient for NOB	0.074	d^{-1}	Wiesmann (1994)
b_{STO}	Aerobic respiration rate of X_{STO}	0.25	d^{-1}	Henze et al. (2000)
K_{OH}	Oxygen half-saturation coefficient for heterotrophs	0.2	g O_2·m^{-3}	Henze et al. (2000)
K_{OA}	Oxygen half-saturation coefficient for AOB	0.3	g O_2·m^{-3}	Wiesmann (1994)
K_{ON}	Oxygen half-saturation coefficient for NOB	1.1	g O_2·m^{-3}	Wiesmann (1994)
K_S	Org. Mat. Half-saturation coefficient for heterotrophs	2	g COD·m^{-3}	Henze et al. (2000)
K_{STO}	X_{STO} half-saturation coefficient for heterotrophs	1	g COD_{STO}·(g COD_{XH})$^{-1}$	Henze et al. (2000)
K_{NO2}	NO_2 half-saturation coefficient for denitrifying heterotrophs	0.5	g NO_2-N·m^{-3}	Vázquez-Padín et al. (2010)
K_{NO3}	NO_3 half-saturation coefficient for denitrifying heterotrophs	0.5	g NO_3-N·m^{-3}	Vázquez-Padín et al. (2010)
K_{NH_A}	Ammonia half-saturation coefficient for AOB	5.71	g NH_4-N·m^{-3}	Wiesmann (1994)
K_{NH_HB}	Ammonia half-saturation coefficient for heterotrophs	0.05	g NH_4-N·m^{-3}	Hauduc et al. (2010)
K_{NO2N}	NO_2 half-saturation coefficient for NOB	0.001	kg NO_2-N·m^{-3}	Vázquez-Padín et al. (2010)
k_{STO}*	Storage rate constant	6.16	g COD_{Ss}·(g COD_{XH})$^{-1}$·d^{-1}	Henze et al. (2000)
k_{STO}	Storage rate constant	**8**	g COD_{Ss}·(g	Calibrated – this study

			$COD_{XH})^{-1}\cdot d^{-1}$	
η_g	Corrector factor for μ_H under anoxic conditions	0.6	-	Henze et al. (2000)
k_h	Maximum specific hydrolysis rate	3.69	g $COD_{sd}\cdot$(g COD_{cell}/day)$^{-1}$	Henze et al. (2000)
K_X	Half-saturation coefficient for hydrolysis of slowly biodegradable substrate	1	g $COD_{sd}\cdot$(g $COD_{cell})^{-1}$	Henze et al. (2000)
$K_{Inh,H}$	Salinity inhibition constant for heterotrophs	44.3	g NaCl.m^{-3}	This study
$K_{Inh,A}$	Salinity inhibition constant for AOB	24.8	g NaCl.m^{-3}	This study
$K_{Inh,N}$	Salinity inhibition constant for NOB	21.7	g NaCl.m^{-3}	This study

*Default values used as a first step during the calibration of the model.

The kinetic parameters were corrected taking into account the operation temperature, as suggested by Hauduc et al., (2010), with Eq.4.

$$k(T) = k(20°\text{C}) \cdot \theta_{pow}{}^{T-20} \quad \text{(Eq.4)}$$

Where k(T) is the kinetic parameter corrected to the working temperature, k(20°C) is the value of the kinetic parameter at 20 °C, T is the temperature (°C) and θ_{pow} is calculated from Eq. 5:

$$\theta_{pow} = \left(\frac{k(T_1)}{k(T_2)}\right)^{1/(T_1 - T_2)} \quad \text{(Eq.5)}$$

The values of k(T1) and k(T2) corresponded to the values of the kinetic parameters from ASM3 at 10 and 20 °C.

Appendix A.3: salinity inhibition

Overview

An overview of various non-competitive inhibition models proposed in literature is given in Table S.6.

Table S.6: Non-competitive inhibition models reported in literature. $K_{Inh,50}$ is the 50% inhibition constant, $K_{Inh,100}$ is the 100% inhibition constant, and S_{Inh} is the inhibitor concentration. K_{IL} (100% inhibition constant), m, n and b are other model constants.

Inhibition term	Inhibitor	Affected bacteria	Reference
(1) $\frac{K_{Inh,50}}{K_{Inh,50}+S_{Inh}}$	Free nitrous acid	AOB	Jiménez et al. (2012) Torà et al. (2010)
	Fluoride	AOB	Carrera et al. (2003)
	Chloramphenicol	Anammox	Phanwilai et al. (2020)
	Cadmium and cooper	HB	Pai et al. (2009)
	Benzene, toluene, phenol, benzoate	Anammox	Peng et al. (2018)
(2) $1-\frac{S_{Inh}}{K_{Inh,100}}$	Salinity	HB Yeast	Dan et al. (2003)
(3) $\frac{K_{Inh,50}}{{S_{Inh}}^{m}+K_{Inh,50}}$	Benzene, toluene, phenol, benzoate	Anammox	Peng et al. (2018)
(4) $1-\left(S_{Inh}/K_{IL}\right)^{n}$	Benzene, toluene, phenol, benzoate	Anammox	Peng et al. (2018)
	Aromatic substances	Anammox	Ramos et al. (2015)
(5) $1-\frac{1}{1+\left(S_{Inh}/K_{Inh,50}\right)^{b}}$	Quinoline	Anammox	Chen et al. (2019)
	Nanoparticles	Anammox	Song et al. (2018)
	Copper	Denitrifying bacteria	Chen et al. (2016)

Estimation of the inhibition constants

The figures corresponding to the reduction of the biological activity associated to the increase of the salt concentrations in biofilms non-adapted to salinity are shown in Figure S.1.

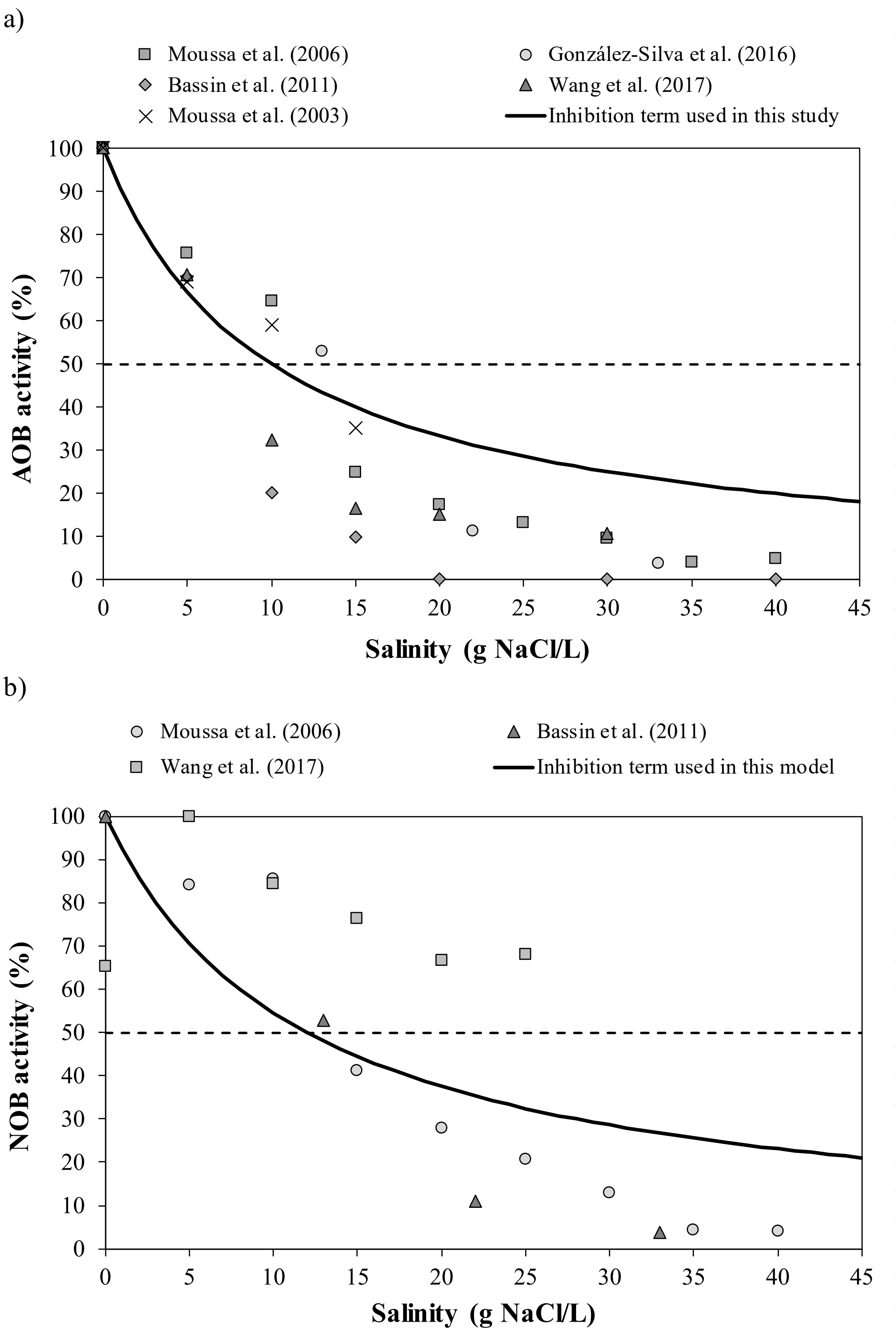

Figure S.1: (a) AOB activity with different salt concentrations of biomass non-adapted to salinity. (b) NOB activity with different salt concentrations of biomass non-adapted to salinity.

Appendix A.4: model calibration results

ASM1

Firstly, the results of the ASM1 calibration are shown (Figure S.2). The figure corresponds to the calibration step with a maximum growth rate of heterotrophs of 20 d^{-1}. The kinetic parameters of both AOB and NOB were not calibrated.

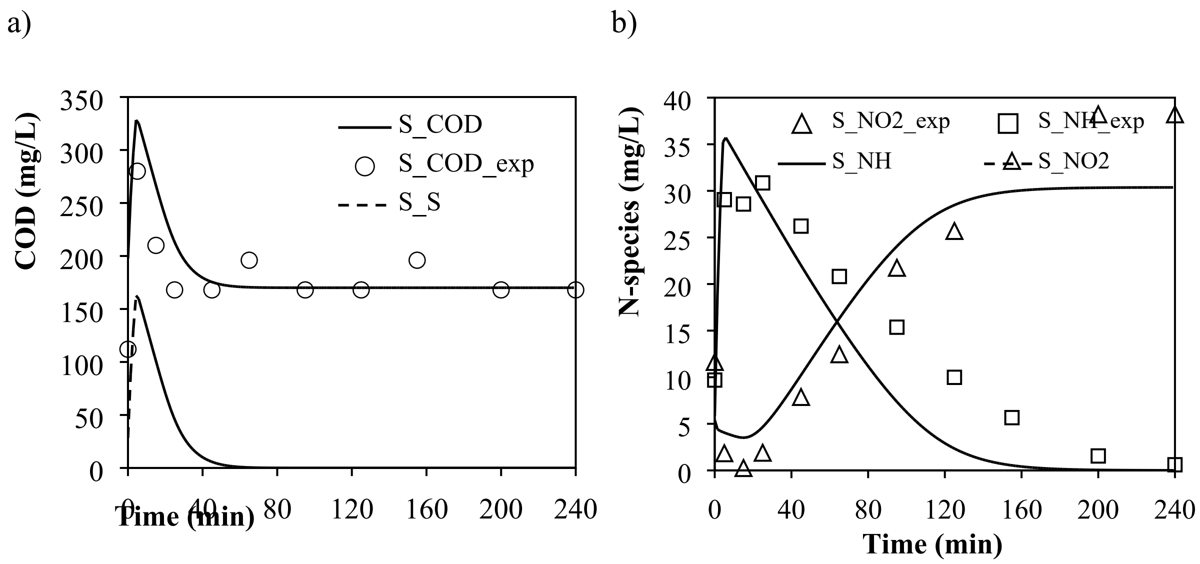

Figure S.2: (a) S_{COD} and S_S profiles predicted with ASM1; and S_{COD} profile from experimental data. (b) S_{NH} and S_{NO2} profiles predicted with ASM1; and S_{NH} and S_{NO2} profiles from experimental data. The experimental data corresponds to a reactor cycle profile measurement performed during the operational phase III.b (salinity of 13 g NaCl/L).

ASM3

Figure S.3 shows the spatial distribution of each type of bacterial population in the granule. It corresponds to the calibrated ASM3.

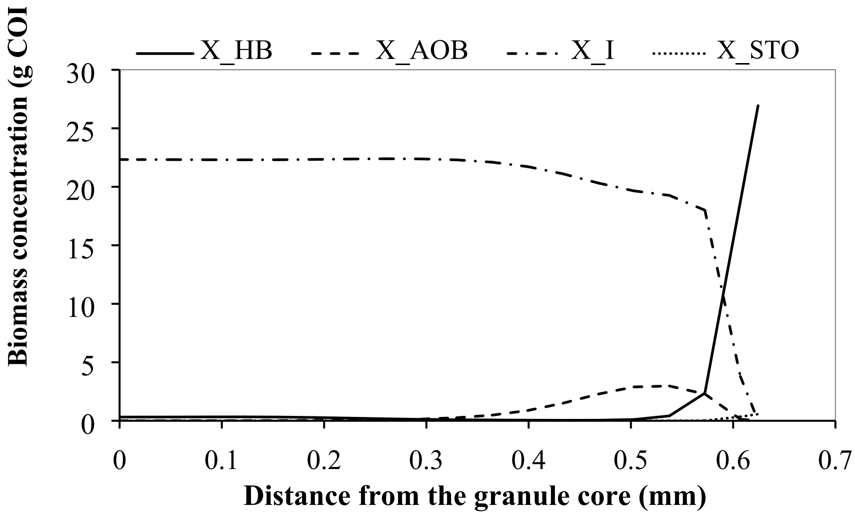

Figure S.3: X_H, X_A, X_{STO} and X_I distribution in the granule predicted by the modified ASM3.

REFERENCES

Beun, J.J., Van Loosdrecht, M.C.M., Heijnen, J.J., 2002. Aerobic granulation in a sequencing batch airlift reactor. Water Res. https://doi.org/10.1016/S0043-1354(01)00250-0

Carrera, J., Baeza, J.A., Vicent, T., Lafuente, J., 2003. Biological nitrogen removal of high-strength ammonium industrial wastewater with two-sludge system. Water Res. https://doi.org/10.1016/S0043-1354(03)00338-5

Carrera, P., Campo, R., Méndez, R., Di Bella, G., Campos, J.L., Mosquera-Corral, A., Val del Rio, A., 2019. Does the feeding strategy enhance the aerobic granular sludge stability treating saline effluents? Chemosphere. https://doi.org/10.1016/j.chemosphere.2019.03.127

Chen, H., Chen, Q.Q., Jiang, X.Y., Hu, H.Y., Shi, M.L., Jin, R.C., 2016. Insight into the short- and long-term effects of Cu(II) on denitrifying biogranules. J. Hazard. Mater. https://doi.org/10.1016/j.jhazmat.2015.11.012

Chen, Q.Q., Xu, L.Z.J., Zhang, Z.Z., Sun, F.Q., Shi, Z.J., Huang, B.C., Fan, N.S., Jin, R.C., 2019. Insight into the short- and long-term effects of quinoline on anammox granules: Inhibition and acclimatization. Sci. Total Environ. https://doi.org/10.1016/j.scitotenv.2018.09.285

Cristóvão, R.O., Pinto, V.M.S., Martins, R.J.E., Loureiro, J.M., Boaventura, R.A.R., 2016. Assessing the influence of oil and grease and salt content on fish canning wastewater biodegradation through respirometric tests. J. Clean. Prod. 127, 343–351. https://doi.org/10.1016/j.jclepro.2016.04.057

Dan, N.P., Visvanathan, C., Basu, B., 2003. Comparative evaluation of yeast and bacterial treatment of high salinity wastewater based on biokinetic coefficients. Bioresour. Technol. https://doi.org/10.1016/S0960-8524(02)00204-3

De Kreuk, M.K., Picioreanu, C., Hosseini, M., Xavier, J.B., Van Loosdrecht, M.C.M., 2007. Kinetic model of a granular sludge SBR: Influences on nutrient removal. Biotechnol. Bioeng. https://doi.org/10.1002/bit.21196

Hauduc, H., Rieger, L., Takács, I., Héduit, A., Vanrolleghem, P.A., Gillot, S., 2010. A systematic approach for model verification: Application on seven published activated sludge models. Water Sci. Technol. https://doi.org/10.2166/wst.2010.898

Henze, M., Gujer, W., Mino, T., Loosdrecht, M. van, 2000. Activated Sludge Models ASM1, ASM2, ASM2d and ASM3 IWA Scientific and Technical Report No.9, Journal of Chemical Information and Modeling. https://doi.org/10.1017/CBO9781107415324.004

Henze, M., van Loosdrecht, M.C.M., Ekama, G.A., Brdjanovic, D., 2008. Biological Wastewater Treatment: Principles, Modelling and Design. https://doi.org/10.2166/9781780401867

Jiménez, E., Giménez, J.B., Seco, A., Ferrer, J., Serralta, J., 2012. Effect of pH, substrate and free nitrous acid concentrations on ammonium oxidation rate. Bioresour. Technol. https://doi.org/10.1016/j.biortech.2012.07.079

Pai, T.Y., Wang, S.C., Lo, H.M., Chiang, C.F., Liu, M.H., Chiou, R.J., Chen, W.Y., Hung, P.S., Liao, W.C., Leu, H.G., 2009. Novel modeling concept for evaluating the effects of cadmium and copper on heterotrophic growth and lysis rates in activated sludge process. J. Hazard. Mater. https://doi.org/10.1016/j.jhazmat.2008.11.009

Peng, S., Han, X., Song, F., Zhang, L., Wei, C., Lu, P., Zhang, D., 2018. Inhibition of benzene, toluene, phenol and benzoate in single and combination on Anammox activity: implication to the denitrification–Anammox synergy. Biodegradation. https://doi.org/10.1007/s10532-018-9853-x

Phanwilai, S., Piyavorasakul, S., Noophan, P. (Lek), Daniels, K.D., Snyder, S.A., 2020. Inhibition of anaerobic ammonium oxidation (anammox) bacteria by addition of high and low concentrations of chloramphenicol and comparison of attached- and suspended-growth. Chemosphere. https://doi.org/10.1016/j.chemosphere.2019.124570

Ramos, C., Fernández, I., Suárez-Ojeda, M.E., Carrera, J., 2015. Inhibition of the anammox activity by aromatic compounds. Chem. Eng. J. https://doi.org/10.1016/j.cej.2015.05.071

Song, Y.X., Chai, L.Y., Tang, C.J., Xiao, R., Li, B.R., Wu, D., Min, X.B., 2018. Influence of ZnO nanoparticles on anammox granules: The inhibition kinetics and mechanism analysis by batch assays. Biochem. Eng. J. https://doi.org/10.1016/j.bej.2018.02.006

Torà, J.A., Lafuente, J., Baeza, J.A., Carrera, J., 2010. Combined effect of inorganic carbon limitation and inhibition by free ammonia and free nitrous acid on ammonia oxidizing bacteria. Bioresour.

Technol. https://doi.org/10.1016/j.biortech.2010.03.005

Vázquez-Padín, J.R., Mosquera-Corral, A., Campos, J.L., Méndez, R., Carrera, J., Pérez, J., 2010. Modelling aerobic granular SBR at variable COD/N ratios including accurate description of total solids concentration. Biochem. Eng. J. https://doi.org/10.1016/j.bej.2009.12.009

Wiesmann, U., 1994. Biological nitrogen removal from wastewater. Adv. Biochem. Eng. Biotechnol. https://doi.org/10.1007/bfb0008736